

# The Recommend of Filler Metal to Increasing the Corrosion Resistance of Gas Pipeline

Esmail Jafari<sup>1\*</sup>, Mohammad Sadegh Karimi<sup>2</sup>

<sup>1</sup>Materials Science and Engineering Dept., Islamic Azad University, Shiraz Branch

<sup>2</sup>Member of South Zagros Oil and Gas Company

\*Email of Corresponding Author: jafarias@iaushiraz.ac.ir

*Received: May 3, 2020; Accepted: August 15, 2020*

## Abstract

The high strength carbon steels such as API X65 is widely used to build the pipelines. In this study, the corrosion behavior welds region of the gas pipeline was studied. For this purpose, Shield Metal Arc Welding (SMAW) was used to evaluate the proposed method. The welding processes were performed with E6010, E6013, and ER70S-6 electrodes as filler metal and welding carried out in 3 passes by a single butt welded method. The corrosion behavior was determined in the gas fluid solution at environment temperature using potentiodynamic polarization test. The microstructure of the base metal, weld zone, and heat-affected zone were investigated with optical microscopy. Results show that the microstructure changes that formed during the welding process were correlated with electrochemical results. And the corrosion performance of the weld joints was influenced by the type of filler metal. As the welded sample with ER70S-6 has high corrosion resistance in comparison to other electrodes.

## Keywords

Bone Scaffold, Implant, Additive Manufacturing, Numerical Analysis

## 1. Introduction

The corrosion phenomena are well-known in the petroleum industry and cause maximum damage to oilfield equipment. Welding is one of the most important processes for fabricating metallic structures. Corrosion failure of welds occurs in spite of the fact that the proper base metal and filler metal have been selected, industry codes and standards have been followed, and welds have been deposited that possess a full weld penetration and have the proper shape and contour. It is not unusual to find that, although the wrought form of a metal or alloy is resistant to corrosion in a particular environment, the welded counterpart is not [1-5].

The pipeline failures usually occur from pitting or galvanic corrosion of welds. Corrosion failures are caused by the local differences in composition and microstructure of the weld metal and base metal. The corrosion failures in the transmission pipeline sector were due to pitting corrosion and galvanic corrosion of weld metal, therefore, it is crucial to improve the corrosion resistance of weld metals [4,5].

The weld metal metallurgy for low alloy steel differs significantly from the base metal metallurgy in several aspects. During welding, thermal cycle heating and cooling rates of the weld are much faster than those of steel base metal. Thus metallurgical transformations across the weld and heat-affected zone vary, thereby their microstructures and morphologies become

important. The microstructures that develop during the welding thermal cycle are dependent on energy input, preheat, metal thickness (heat sink effect), weld bead size, and reheating effects due to multi-pass weld. As a result of different chemical compositions and inclusions weld metal microstructures significantly differs from those of the HAZ and base metal, corrosion behavior can also change [6,7]. Therefore, the welding process has a significant influence on corrosion resistance and mechanical properties as a result of metallurgical changes involved.

A different electrochemical potential gradient is developed in adjacent sites of a weld metal because of these microstructure changes, therefore research work was directed towards the study of corrosion behavior of welded microstructures [8,9].

It is well known that the alloying elements of Ni, Cu, Cr, and Mo contribute to the corrosion resistance of Fe-based alloys, but this is not a good way to join the alloying elements in the filler metal regardless of the cost in the industrial manufacture. Therefore, this work proposes a recommend filler metal design to minimize corrosion. The objective of the present study is to investigate the influence of filler metal type on the corrosion behavior of carbon steel grade X65 in the three different weld regions (base metal (BM), weld zone (WZ), and heat-affected zone (HAZ) in the gas fluid solution.

## 2. Experimental procedure

### 2.1 Materials preparation

The low-carbon steel specimens ( $20 \times 20 \times 8$  mm), Grade X65, with a composition in wt.% were: (Fe: base, Mn: 1.645, Si: 0.45, C: 0.16, Al: 0.02, Mo: 0.01, Cr: 0.01, S: 0.01, Ti: 0.06, V: 0.08,) have been used in this study. Two plates of pipe were butt-welded by the SMAW welding process at 3 passes using E6010, E6013, and ER70S-6 electrodes as the filler metal. The composition of the electrodes is shown in Table 1. In all specimens, were fixed current and voltage and changed the type of electrode. Three different specimens were prepared for electrochemical corrosion testing. The Characteristics of specimens are given in Tables 2.

Table.1. Composition of the filler metals

<b>Composition</b>	<b>C%</b>	<b>Mn%</b>	<b>P%</b>	<b>S%</b>	<b>Cu%</b>	<b>Ni%</b>	<b>Si%</b>
<b>E6013</b>	0.08	0.45	0.012	0.009	----	0.01	0.18
<b>E6010</b>	0.06	1.2	0.013	0.12	----	----	0.5
<b>ER70S-6</b>	0.09	1.7	0.025	0.025	0.5	0.15	1

Table. 2. Characteristics of specimens

<b>Welding number</b>	<b>Type of Electrode</b>	<b>Voltage</b>	<b>Passes</b>	<b>Diameter (mm)</b>	<b>Current (A)</b>
<b>W1</b>	E6010	22	First	3.25	90
			Second	3.25	110
			Third	3.25	110
<b>W2</b>	ER70S-6	22	First	1	90
			Second	1	110
			Third	1	110
<b>W3</b>	E6013	22	First	3.25	90
			Second	3.25	110
			Third	3.25	110

### 2.2 Microstructure and Phase Analysis

For microstructure investigation by optical microscopy all samples were cut (cross-sectioned) from the weld Zone, WZ, heat affected zone, HAZ, and base metal, BM. The samples were polished with silicon carbide paper numbers 400 – 600 – 1000 and 1200 respectively. And etching was performed using a solution of nital 2% in 20 seconds.

### 2.3 Electrochemical measurements

The potentiodynamic polarization measurements and cyclic polarization were carried out in a standard three-electrode cell in 500 ml solution with the Ag- AgCl, as the reference electrode, platinum electrode as the auxiliary or counter electrode and the sample as the working electrode by an Autolab potentiostat /galvanostat (PGSTAT30) apparatus. The specimens with the surface area 1 cm<sup>2</sup> were sealed in the epoxy resin. The polarization test was carried out at the open circuit potential (OCP) in the test solution at room temperature. Table 3 was shown the characteristic of the test solution. The corrosion tests consisted of stabilizing the auxiliary electrode in the corrosion test solution at open circuit potential for 3 hours before the test and the test was started at a scan rate of 0.02 mV/S with a range of  $\pm 500$  mV from OCP.

Table.3. Characteristic of the gas fluid solution at environment temperature

<b>NaCl(ppm)</b>	<b>Cl(ppm)</b>	<b>Fe(ppm)</b>	<b>Mn(ppm)</b>	<b>PH</b>
42410	25740	6.3	1	6.67

### 3. Results and discussion

The visual observation of all samples revealed that strong fusion exists between the weld region and the base metals. All the weld joints are continuously showing no significant surface defects. This is an indication that the heat energy inputs available at welding were sufficient for the complete melting of the base metals and the wire electrodes. Therefore the corrosion resistance and weld zone properties depend on the relative proportions and morphologies of these constituents that are formed during the welding process. The metallurgical microstructure of the weldment can be dramatically influenced by the welding materials and welding operations [8-11]. The microstructures of WZ, HAZ, and BM in the welded condition were shown in Figure 1 to 5. According to these Figures, it is determined that the base metal microstructure before welding was completely the austenitic phase. In the shield metal arc welding, the microstructures generally are composed of a complex mixture of microstructure constituents.

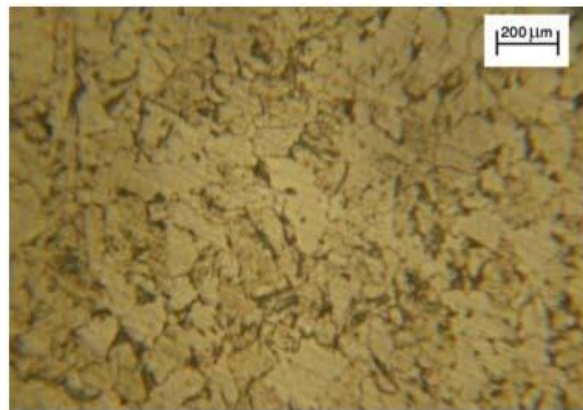


Figure1. The microstructure of base metal before welding

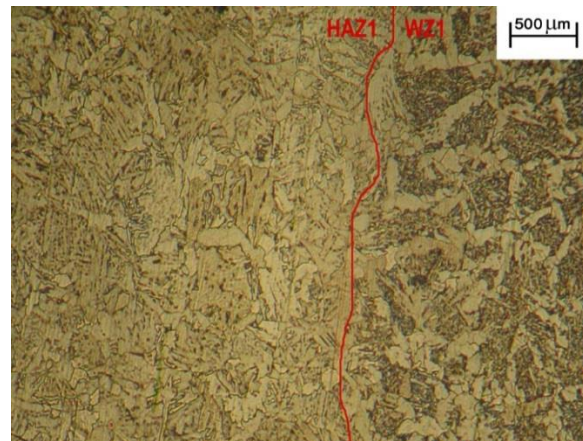


Figure 2. The microstructures variation from HAZ to WZ



Figure 3. The microstructures variation from BM to HAZ

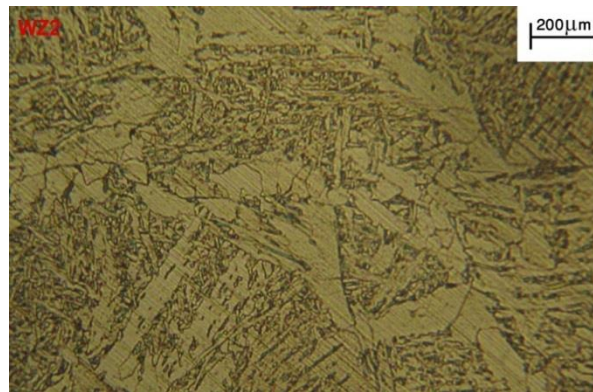


Figure 4. The BM microstructure consisted of equiaxed polygonal ferrite (white phase) and pearlite (black phase) grains

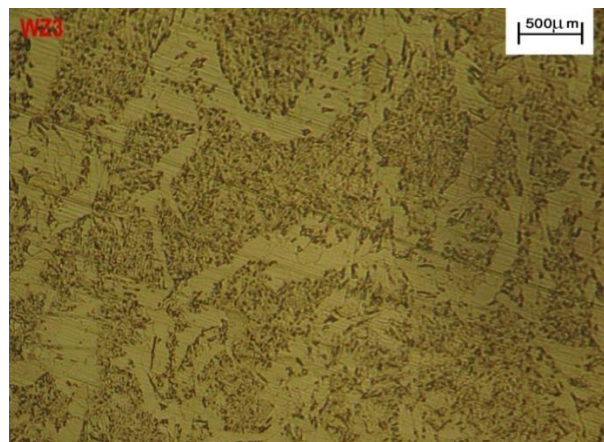


Figure 5. The  $\alpha_w$  microstructure of austenite grain phase in HAZ zone

The BM microstructure consisted of the equiaxed polygonal ferrite (white phase) and pearlite (black phase) grains as shown in Fig. 4. In WZ the microstructure analysis indicated the allotriomorphic ferrite ( $\alpha$ ) as the grain boundary ferrite, wedge shape secondary widmanstatten ferrite ( $\alpha_w$ ) originated from these allotriomorphic and lathlike arrangement of acicular ferrite ( $\alpha_a$ ) that was a characteristic microstructure of upper bainite inside the grain. The  $\alpha_w$  was formed by the para-equilibrium transformation of the austenite grain surface, the detailed microstructure is given in Fig.5. It may be visualized as consisting of two mutually accommodating plates with the characteristic thin wedge morphology of  $\alpha_w$ . The  $\alpha_a$  was a phase, most commonly observed as

austenite transforms during the cooling of low alloy steel weld deposits. The nature of  $\alpha_a$  in the weld metals was the upper bainite having needle-like morphology and this corresponds to mid-temperature phase transformation. Also, the morphology of precipitates was affected by the amount of Ni and Mn in the ER70S-6 filler metal. The high Ni filler metal could improve the corrosion behavior of weld [12 -16].

Figures 6 and 7 show the potentiodynamic polarization curves for, WZ, HAZ, and BM. It is clear that the corrosion resistance of the welding zone of sample one, WZ<sub>1</sub>, is lower than the corrosion resistance of another specimen.

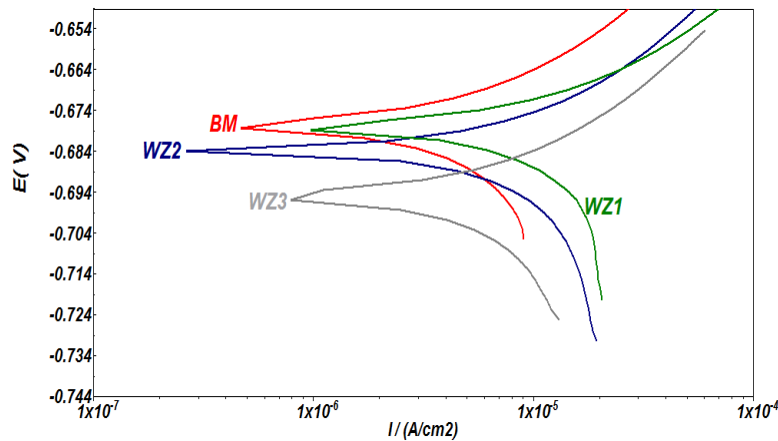


Figure 6. The potentiodynamic polarization curves of WZ and BM

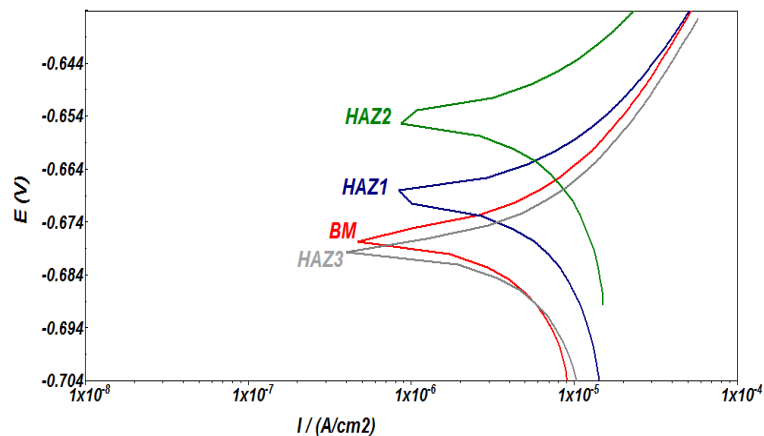


Figure 7. The potentiodynamic polarization curves of HAZ and BM

The polarization curve parameters were obtained by Tafel's extrapolation using the Nova software, as shown in Table 4. According to these results, the WZ<sub>1</sub> specimen has lower polarization resistance and therefore higher corrosion current density ( $i_{\text{corr}} = 9.17 \mu\text{A} \cdot \text{cm}^{-2}$ ) in the gas fluid solution compared with the WZ<sub>2</sub> ( $i_{\text{corr}}=0.59 \mu\text{A} \cdot \text{cm}^{-2}$ ) and WZ<sub>3</sub> ( $i_{\text{corr}} = 7.40 \mu\text{A} \cdot \text{cm}^{-2}$ ) in the same condition. Also, WZ<sub>3</sub>, compared with WZ<sub>1</sub> and WZ<sub>2</sub> has lower open circuit potential. The corrosion potential of WZ<sub>3</sub> is lower than the WZ<sub>1</sub> & WZ<sub>2</sub> and the corrosion rate in the WZ<sub>1</sub> is higher than other specimens. Therefore, WZ<sub>1</sub> has a higher tendency to corrosion. The open-circuit potential or OCP shows in Table 4.

Table 4. Potentiodynamic polarization Results

Welding no.	Position	OCP (mv/sec)	E <sub>corr</sub> (mv)	I <sub>corr</sub> (μA/cm <sup>2</sup> )	R <sub>p</sub> (ohm)	C.R (mm/year)
W1	WZ	-674	-678	9.174	804	0.215
	HAZ	-667	-689	3.75	1187	0.088
W2	WZ	-679	-686	0.593	1316	0.014
	HAZ	-671	-667	4.01	1460	0.0943
W3	WZ	-663	-683	7.40	985	0.173
	HAZ	-659	-655	5.852	1283	0.137
BM	BM	-679	-677	2.778	1774	0.065

These results show that the OCP of the WZ<sub>2</sub> specimen was a little different from the OCP of the WZ<sub>1</sub> specimen. Also, WZ<sub>2</sub> has the lowest  $i_{corr}$  compared to other samples. The slope of the polarization curve in the WZ<sub>2</sub> is less than the other samples. Therefore must expect that polarization resistance in the WZ<sub>2</sub> is greater than the other specimens. The corrosion results of the HAZ<sub>2</sub> in Table 4, also confirm increasing the corrosion resistance of the sample HAZ<sub>2</sub>. From this result can be concluded that the W<sub>2</sub> is higher corrosion resistance with respect to another specimen. The results of the electrochemical study were correlated with microstructure changes that formed during the welding thermal cycle. The higher corrosion potential at the weld joints is as a result of the presence of the higher Ni and Mn content. Therefore, the ER70S-6 can be a more suitable electrode due to the high amount of nickel and manganese in its composition.

The recommend design of the alloying elements in the filler metal can be used as guidelines for the production, and the excellent corrosion resistance in all environments makes the filler metal containing Ni, Cu, and Mn promising for industrial applications. Therefore, it is clear that the ER70S-6 electrode is highly suitable for gas pipeline welding.

#### 4. Conclusion

The influence of filler metal composition on the Corrosion behavior of low-carbon steel, Grade X65 welds was studied. And the corrosion characteristics of the weld zone were investigated using three electrodes for 8 mm-thick-API 5L X65 welded with SMAW in three regions of WZ, HAZ, and BM. Although the filler material with similar chemical composition to the base metal was suggested for welding, the results showed that the application high Mn filler metal the optimum corrosion resistance of Samples. And the as-welded sample with ER70S-6 has high corrosion resistance with comparison to the other electrode in the gas fluid solution.

#### 5. Acknowledgments

This investigation was supported by the Islamic Azad University-Shiraz branch with NIOC – South Zagros Oil & Gas Company Research Department.

#### 6. References

- [1] Yesen, Z., Yunze, X., Mingyu, W., Xiaona, W., Gang, L. and Yi, H. 2019. Understanding the influences of temperature and microstructure on localized corrosion of subsea pipeline weldment using an integrated multi-electrode array. *Ocean Engineering*. 189:1-14.

- [2] Sabet, A. R. and Montazerolghaem, H. 2018. Manufacturing of Aluminum Thin Cylindrical Parts By Using Friction Stir Welding Method, *Journal of Modern Processes in Manufacturing and Production*. 7:21-28
- [3] Moradi, M., Ghoreishi, M. and Rahmani, A. 2016. Numerical and Experimental Study of Geometrical Dimensions on Laser-TIG Hybrid Welding of Stainless Steel 1.4418. *Journal of Modern Processes in Manufacturing and Production*. 5: 21-31
- [4] Granjon, H. *Fundamentals of Welding Metallurgy*. 1991. Abington Publishing. 156-177.
- [5] Aneesh, K. and Prashant, D. 2020. Investigating the effects of filler material and heat treatment on hardness and impact strength of TIG weld. *Materials Today: Proceedings*. 33: 1-7.
- [6] Deen, K. M., Ahmad, R., Khan, I. H. and Farahat, Z. 2010. Microstructural study and electrochemical behavior of low alloy steel weldment. *Materials and Design*. 31 (1), 3051–3055.
- [7] Waqar, H., Masood, U. and Tariqc, M. 2020. Assessment of fatigue and electrochemical corrosion characteristics of dissimilar materials weld between alloy 617 and 12 Cr steel. *Journal of Manufacturing Processes*. 53:275-282.
- [8] Hongyang, J., Yongdian, H., Zhicao, F. and Lianyong, X. 2016. Recommend design of filler metal to minimize carbon steel weldmetal preferential corrosion in CO<sub>2</sub>-saturated oilfield produced water. *Applied Surface Science*. 389: 609-622
- [9] Abioyca, T.E., Ariwoolac, O.E., Ogedengbec, T.I., Farayibib, P.K. and Gbadeyanc, O.O. 2019. Effects of Welding Speed on the Microstructure and Corrosion Behavior of Dissimilar Gas Metal Arc Weld Joints of AISI 304 Stainless Steel and Low Carbon Steel. *Materials Today, Proceedings*, 17(3): 871–877.
- [10] Anbarasu, P., Yokeswaran, R., Godwin, A. and Sivachandran, S. 2020. Investigation of filler material influence on hardness of TIG welded joints. *Materials Today: Proceedings*. 33: 1-4.
- [11] Zhanga, Y., Hongyang, J., Lianyong, X., Yongdian, H. and Lei, Z. 2018. Design and performance of weld filler metal to match an advanced heat resistant Fe-Cr-Ni alloy. *Materials Science & Engineering A*. 721:103-116.
- [12] Liqing, H., Guobiao, L., Zidong, W., Hong, Z., Feng, Li. and Long, You. 2010. Study on Corrosion Resistance of 316L Stainless Steel Welded Joint. *Rare Metal Materials and Engineering*. 3: 393–396.
- [13] Tan, H., Wang, Z., Jiang, Y., Yang, Y., Deng, Bo. and Song, H. 2012. Influence of welding thermal cycles on microstructure and pitting corrosion resistance of 2304 duplex stainless steels. *Corrosion Science*. 55:368–377.
- [14] Yang, Y., Yan, B., Li, J. and Wang, J. 2011. The effect of large heat input on the microstructure and corrosion behavior of simulated heat affected zone in 2205 duplex Stainless Steel. *Corrosion Science*. 53:3756-3763.
- [15] Rudra, P., Pratap, S. and Subodh, K. 2020. Effect of current and chemical composition on the hardness of weld in shielded metal arc welding. *Materials Today: Proceedings*. 26-2:1888-1891.
- [16] Fuyun, L., Caiwang, T., Xiangtao, G., Laijun, W. and Jicai, F. 2020. A comparative study on microstructure and mechanical properties of HG785D steel joint produced by hybrid laser-MAG welding and laser welding. *Optics & Laser Technology*. 128:106247